Nuclear Medicine and Molecular Imaging (2019) 53:189–198
https://doi.org/10.1007/s13139-019-00587-w

ORIGINAL ARTICLE

ISSN (print) 1869-3482
ISSN (online) 1869-3474

Development of a Novel Imaging Agent for Determining Albumin Uptake in Solid Tumors

S. Daum[1] · J. P. Magnusson[1] · L. Pes[1] · J. Garcia Fernandez[1] · S. Chercheja[1] · F. Medda[1] · F. I. Nollmann[1] · S. D. Koester[1] · P. Perez Galan[1] · A. Warnecke[1] · K. Abu Ajaj[1] · Felix Kratz[1]

Received: 13 December 2018 / Revised: 23 January 2019 / Accepted: 23 January 2019 / Published online: 20 February 2019

Abstract

Purpose The purpose of this study was to investigate the albumin-binding compound ^{111}In-C4-DTPA as an imaging agent for the detection of endogenous albumin accumulation in tumors.

Methods ^{111}In-C4-DTPA was injected in healthy nude mice for pharmacokinetic and biodistribution studies (10 min, 1, 6, 24, and 48 h, $n = 4$) and subsequently in tumor-bearing mice for single-photon emission computed tomography/X-ray-computed tomography (SPECT/CT) imaging studies. Four different human tumor xenograft models (LXFL529, OVXF899, MAXFTN401, and CXF2081) were implanted subcutaneously unilaterally or bilaterally ($n = 4$–8). After intravenous administration of ^{111}In-C4-DTPA, SPECT/CT images were collected over 72 h at 4–6 time points. Additionally, gamma counting was performed for the blood, plasma, lungs, heart, liver, spleen, kidneys, muscle, and tumors at 72 h post-injection.

Results ^{111}In-C4-DTPA bound rapidly to circulating albumin upon injection, and the radiolabeled albumin conjugate thus formed was stable in murine and human serum. SPECT/CT images demonstrated a time-dependent uptake with a maximum of 2.7–3.8% ID/cm^3 in the tumors at approximately 24 h post-injection and mean tumor/muscle ratios in the range of 3.2–6.2 between 24 and 72 h post-injection. The kidneys and bladder were the predominant elimination organs. Gamma counting at 72 h post-injection showed 1.3–2.5% ID/g in the tumors and mean tumor/muscle ratios in the range of 4.9–9.4.

Conclusion ^{111}In-C4-DTPA bound rapidly to circulating albumin upon injection and showed time-dependent uptake in the tumors demonstrating a potential for clinical application as a companion imaging diagnostic for albumin-binding anticancer drugs.

Keywords Albumin · Drug carrier · Imaging agent · SPECT/CT imaging · Tumor accumulation · ^{111}In

Introduction

Various drug carrier systems are being developed to optimize the site-specific delivery of anticancer drugs and to reduce side effects in healthy tissues [1]. An effective method for improving the therapeutic index of anticancer drugs is to conjugate these with a macromolecule, such as serum albumin [2]. Albumin, the most abundant plasma protein, has a half-life of ~ 19 days in humans. Albumin demonstrates a preferential tumor uptake in various tumor models due to the enhanced permeability and retention of macromolecules in solid tumors, a phenomenon commonly known as the enhanced permeability and retention (EPR) effect, which is due to enhanced angiogenesis combined with a leaky vasculature and a defective lymphatic drainage system [2, 3]; in addition, several albumin-binding proteins are present in the tumor environment, such as SPARC and albondin (gp60) [4].

During the past two decades, we have successfully investigated a tumor-targeting approach in which maleimide-bearing prodrugs exploit endogenous albumin as a drug carrier. This macromolecular prodrug concept is based on two features: (a) rapid and selective binding of a maleimide-containing prodrug to the cysteine-34 residue of endogenous

S. Daum and J. P. Magnusson contributed equally to this work.

Electronic supplementary material The online version of this article (https://doi.org/10.1007/s13139-019-00587-w) contains supplementary material, which is available to authorized users.

✉ Felix Kratz
fkratz@centurionbiopharma.com; fkratz@cytrx.com

[1] Centurion Biopharma Corporation/CytRx Drug Discovery Branch, Engesserstr. 4, 79108 Freiburg, Germany

albumin after intravenous administration, and (b) release of the albumin-bound drug predominantly at the tumor site due to the incorporation of a cleavable bond (hydrolytically, reductively, enzymatically, and/or acid-sensitive) between the drug and the carrier [1, 2, 5–8]. Cysteine-34 is the only cysteine residue of serum albumin with a free sulfhydryl group which does not participate in interchain disulfide linkage. The X-ray structure of defatted albumin reveals that cysteine-34 is located in a crevice on the surface of subdomain IA of albumin that is approximately 10–12 Å deep [9]; the crevice opens up when fatty acids are bound to the five binding sites as is the case in blood circulation rendering it more accessible [6]. This free HS-group is an unusual feature of an extracellular protein and is a readily accessible functional group that can be used for in situ conjugation of thiol-reactive drugs with circulating albumin after intravenous administration, thereby generating a macromolecular drug delivery system in the blood stream [6].

In situ binding of maleimide-based prodrugs to circulating albumin is a preclinically and clinically validated approach for increasing the therapeutic index of anticancer agents. An acid-sensitive anthracycline prodrug, the (6-maleimidocaproyl)hydrazone derivative of doxorubicin (aldoxorubicin, previously named DOXO-EMCH or INNO-206), has undergone extensive clinical testing [8, 10, 11] and has shown significantly improved response rates and progression-free survival over the parent drug doxorubicin in a phase 2b randomized clinical trial for first-line treatment of soft tissue sarcoma [11]. Similar results with aldoxorubicin against investigators' choice of five optional drugs were obtained in a phase 3 clinical trial for second-line treatment of L-sarcomas [10]. Aldoxorubicin therapy exhibited manageable adverse effects without unexpected events and, importantly, without evidence of acute cardiotoxicity [10].

The clinical application of albumin-binding prodrugs would greatly benefit if the extent of albumin uptake in malignant tumors and in metastatic lesions could be determined. The development of an imaging agent that is capable of quantifying the uptake of albumin in the tumor of patients would therefore facilitate the selection of patients for therapy with albumin-binding drugs such as aldoxorubicin. Patients showing high tumor accumulation of the companion diagnostic imaging agent would therefore be more likely to benefit from such treatment. Clinically, radiolabeled albumin has been already used as a diagnostic tool in the form of ^{99m}Tc-aggregated albumin such as ^{99m}Tc-Albures (200–100 nm in diameter) and ^{99m}Tc-Nanocoll (~ 8 nm in diameter) primarily for whole-body lymphoscintigraphy and/or sentinel lymph node detection [12, 13].

For our purpose, however, we needed to develop a different albumin-labeling approach that mimics our proprietary drug delivery technology for imaging solid tumors. Thus, we opted to combine a maleimide-bearing linker with the chelating agent diethylenetriaminepentaacetic acid (DTPA) for our SPECT imaging agent since DTPA is known to readily form a stable complex with the radionuclide ^{111}In. Several ^{111}In-DTPA-based imaging agents have been developed and are already approved for medical use, some of which are used in oncology [14, 15].

In this work, we describe the synthesis of a maleimide-bearing chelating agent and present SPECT/CT data demonstrating distinct uptake of radiolabeled albumin in subcutaneously implanted tumors in nude mice.

Materials and Methods

pH measurements were performed with a pH meter WTW Inolab 7310 with SenTix® mic-D electrodes. Centrifugation was carried out using an Eppendorf centrifuge 5810 R (refrigerated) with a Rotor A-4-81, 230 V/50–60 Hz. Lyophilization was carried out using a Martin Christ Alpha or Epsilon 2-4 LSCplus freeze drier. Mass spectra were collected on a Bruker AmaZon SL (LRMS-ESI) or Thermo Fisher LCQ advantage (LRMS-ESI) spectrometer. HPLC was performed using a Shimadzu Nexera XR HPLC system equipped with a SPD-M20A photodiode array detector.

DMSO was used in anhydrous form unless otherwise stated (Sigma-Aldrich). Water was used from a Direct-Q® 3 UV water purification system (Merck Chemicals GmbH, Schwalbach, Germany). All solvents for synthesis including HPLC and LC-MS grade solvents were purchased from Carl Roth unless otherwise stated. Acetonitrile HPLC grade was purchased from AppliChem GmbH.

The synthesis and lyophilization and radiolabeling protocols for the maleimide-bearing DTPA chelating agent, C4-DTPA, and its albumin conjugate, C4-DTPA-Albumin, are described in the Supplementary Material.

Albumin-Binding and Stability Studies with ^{111}In-C4-DTPA in Human and Murine Serum

Murine serum was obtained from naïve NMRI nu/nu mice. Blood was drawn via cardiac puncture and transferred into vials and kept at room temperature for 30 min. Serum was separated by centrifugation, 2000*g* for 10 min at room temperature, aliquoted, and snap-frozen in liquid nitrogen. The serum was stored at − 80 °C.

Human serum, type AB (male), from clotted whole blood (Sigma-Aldrich) was kept frozen and brought to room temperature, spun down at 13.6 kRPM for 60 s, and filtered through a 0.45-μm syringe filter before use.

Human or NMRI murine serum was incubated at 37 °C before being mixed in 1:30 ratio (*v*:*v*) with ^{111}In-C4-DTPA (57.7 ± 0.7 MBq). Samples were taken at different time points

(1 min, 5 min, and 30 min, additionally 24 h and 48 h for murine serum samples) and analyzed by radio-HPLC. The concentrations of free ^{111}In, unbound ^{111}In-C4-DTPA, and ^{111}In-C4-DTPA-Albumin conjugate were determined in each measurement by HPLC radiographs as depicted in Fig. 1S of the Supplementary Material. Binding to albumin in the serum was determined by comparing the area under the curve (AUC) for each measurement to that of ^{111}In-C4-DTPA in water. The rate of binding of ^{111}In-C4-DTPA to albumin and the stability of the albumin conjugates are presented in Fig. 2S in the Supplementary Material.

Animals and Ethical Statement

All animal procedures were performed according to the German Animal Protection Law or National Institute of Health (NIH) guidelines and approved by the National Animal Experiment Board, Finland. Animal studies were performed with female immunodeficient NMRI nude mice (Charles River Discovery Research Services Germany GmbH, Freiburg, Germany). All animals were group-housed in cages under standard conditions (temperature 22 ± 1 °C, 13-h light/11-h dark, ad libitum food and water) at Charles River, Kuopio, Finland.

In Vivo Biodistribution Study

A total of 40 NMRI mice 8–10 weeks old were dosed intravenously with the imaging agent ^{111}In-C4-DTPA (6.2 ± 0.1 MBq) or with the radiolabeled conjugate ^{111}In-C4-DTPA-Albumin (6.0 ± 0.3 MBq) serving as a comparison. An injection volume of 100 μL was prepared by mixing 35 μL of radiolabeled metal complex and 65 μL of sterile saline (B. Braun). Samples were collected at 10 min, 1 h, 6 h, 24 h, and 48 h after intravenous dosing ($n = 4$ for each time point for each compound). At the specified time points, the mice were euthanized with CO_2, and a blood sample was drawn via cardiac puncture. A small volume of blood was pipetted into a separate tube, and the remaining blood sample was stored on ice until plasma separation. Plasma was separated by centrifugation (2000*g* for 10 min at 4 °C). Additionally, samples from the lungs, heart, liver, spleen, kidneys, and muscle (quadriceps) were collected into pre-weighted tubes. After sample collection, the tubes were weighed again, and the radioactivity was measured with a gamma counter (Wizard II, Perkin Elmer). The data is presented as percentages of the injected dose per gram of tissue (% ID/g).

In Vivo SPECT/CT Imaging of Tumor-Bearing Mice

Female immunodeficient NMRI nude mice received unilateral or bilateral subcutaneous patient-derived (PDX) tumor implants in the flanks while under isoflurane anesthesia at the Charles River site in Freiburg, Germany. SPECT/CT imaging studies were performed in four human tumor xenograft models: LXFL529 (non-small cell lung cancer), OVXF899 (ovarian cancer), MAXFTN401 (mammary carcinoma), and CXF2081 (colorectal cancer). The body weight and tumor size of the tumor-bearing mice were measured daily. Injection with the radiolabeled imaging agent and subsequent imaging studies (Charles River, Kuopio, Finland) were started when the individual tumors were palpable and had reached a volume of 100–300 mm^3. The mice were anesthetized and injected intravenously with a solution of ^{111}In-C4-DTPA (31.0 ± 1.4 MBq) via the tail vein. SPECT/CT imaging was performed with a small animal SPECT/CT (NanoSPECT/CT Plus, Mediso) at 0–1 h, 24 h, 48 h, and 72 h post-dosing. 2D and 3D images of the animals combined with CT were produced to visualize the biodistribution of the labeled agent. The imaging protocol consists of a planar tomography image which was used as a reference to choose the imaging area (tumors are in the center of the field of view). Of note, due to spatial constraints in the imaging chamber, SPECT/CT was focused on the tumor implanted in the left flank. After selecting the imaging area, helical CT was performed (180 projections, 55 kVp, 750-ms exposure time). Finally, helical SPECT scans were performed from the same coordinates using 90 s/time frame. High-resolution multipinhole apertures were used to enhance the resolution. After SPECT/CT imaging, HiSPECT reconstruction was used for the SPECT images. Image analysis was performed using PMOD software v3.7. After the 72-h imaging time point, the mice were euthanized with CO_2. A blood sample was drawn via cardiac puncture. The chest cavity was opened, and small volumes of blood were collected into separate tubes and the remaining blood samples stored on ice until plasma separation. Plasma was separated by centrifugation, 2000*g* for 10 min at 4 °C. Samples from the lungs, heart, liver, spleen, kidneys, muscle (quadriceps), and tumors were collected into pre-weighted tubes. After sample collection, the tubes were weighed again, and the radioactivity was measured with a gamma counter (Wizard II, Perkin Elmer). For the tumor models LXFL529 and OVXF899 ($n = 8$), half of the mice ($n = 4$) were subjected to transcardial perfusion with heparinized saline before sample collection. The samples from the remaining four mice were collected without perfusion. Data are presented as percentages of the injected dose per gram of tissue (% ID/g). Statistical analyses were performed with GraphPad Prism bioanalytic software.

Results

Structural Design and Syntheses of Imaging Agent

The general chemical structure of the precursor for the imaging agents was designed to contain a maleimide group as an

albumin-binding moiety and the acyclic chelating agent diethylenetriaminepentaacetic acid (DTPA), which can bind a wide range of metals including clinically used gamma-emitting radioisotopes for SPECT such as ^{111}In, ^{67}Ga, and ^{99m}Tc [16]. For this study, we selected ^{111}In as a widely used radionuclide for SPECT imaging which has a half-life of 2.8 days.

In designing the imaging agent, we opted for a straightforward synthetic procedure and a length of the maleimide linker of ~ 11 Å (Fig. 1a) that would show an ideal fit for the 10–12-Å deep cavity of the cysteine-34 albumin pocket [6]. The chelating agent, C4-DTPA, was synthesized in a one-step synthesis using an established coupling method by reacting the DTPA derivative *p*-NH_2-Benzyl-DTPA·4 HCl with a pre-activated maleimide carboxylic acid (Fig. 1a) and was obtained as a white solid in a yield of 22% after chromatographic purification.

Radiochemical Labeling

The imaging agent ^{111}In-C4-DTPA was produced from radiolabeling its precursor C4-DTPA (Fig. 1b) with $^{111}InCl_3$ in HCl solution (see Fig. 1S—Supplementary Material). No free ^{111}In was present, but the radio peak showed a shoulder which can be explained by the formation of diastereomeric indium-DTPA complexes in accordance with Schmitt-Willich et al. [17] after complexation. The labeling was reproducible and the radiochemical purity of the ^{111}In-C4-DTPA peak was 98.7–99.4% (Fig. 1Sb).

Albumin-Binding Properties of the Imaging Agent ^{111}In-C4-DTPA

The albumin-binding properties of ^{111}In-C4-DTPA were studied in vitro in both human and murine serum using a RP-HPLC with a radio detector. No free ^{111}In-C4-DTPA was observed after addition to either human or murine serum, but a new radioactive peak was rapidly observed which corresponded to the albumin conjugate (^{111}In-C4-DTPA-Albumin) demonstrating spontaneous albumin binding. ^{111}In-C4-DTPA binding to both murine and human serum albumin was complete within 1 min (Fig. 2Sa and 2Sb—Supplementary Material). HPLC stability studies over an observation period of 30 min in human serum and 48 h in mouse serum showed no decrease of albumin-bound ^{111}In-C4-DTPA (Fig. 2Sc and 2Sd—Supplementary Material).

Pharmacokinetics and Biodistribution Study of ^{111}In-C4-DTPA and ^{111}In-C4-DTPA-Albumin Conjugate in NMRI Mice

After confirming the rapid in vitro binding of the imaging agent ^{111}In-C4-DTPA to albumin, the subsequent step was to study its biodistribution in healthy nude mice following i.v. injection. As a rational comparator, the ex vivo conjugate ^{111}In-C4-DTPA-Albumin, prepared from binding C4-DTPA to exogenous human serum albumin and subsequent labeling with radioactive ^{111}In, was administered to a second group of healthy mice. For biodistribution studies, the mice ($n = 4$) were sacrificed at different time points (10 min, 1 h, 6 h, 24 h, and 48 h after i.v. dosing), and the radioactivity of the radiolabeled albumin in the blood, plasma, and healthy organs was determined by gamma counting. A comparison of the biodistribution profile over 48 h between the albumin-binding agent ^{111}In-C4-DTPA and the ex vivo albumin conjugate ^{111}In-C4-DTPA-Albumin showed very similar radioactivity intensities in the blood and plasma underscoring a comparable pharmacokinetic profile (Fig. 2). Biodistribution profiles in the kidneys, muscle, heart, and lung of ^{111}In-C4-DTPA and ^{111}In-C4-DTPA-Albumin were essentially identical, but different profiles in liver and spleen were recorded (Fig. 2). In summary, based on the results of the binding and stability results as well as the biodistribution study and the ease of synthesis compared to the ex vivo prepared conjugate, the albumin-binding imaging agent ^{111}In-C4-DTPA was selected for further SPECT/CT imaging in tumor-bearing nude mice models.

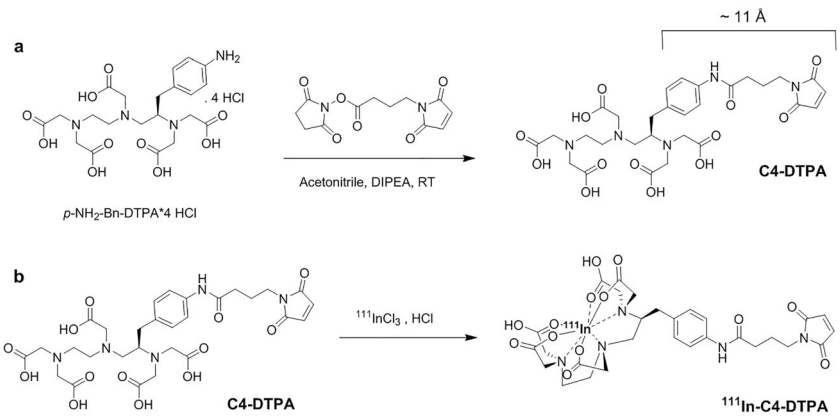

Fig. 1 **a** Synthesis of the maleimide-bearing chelating agent C4-DTPA. The maleimide linker has a length of ~ 11 Å as determined with the software program ChemBio3D Pro, Version 14.0.0.117 (PerkinElmer). **b** Synthesis of ^{111}In-C4-DTPA

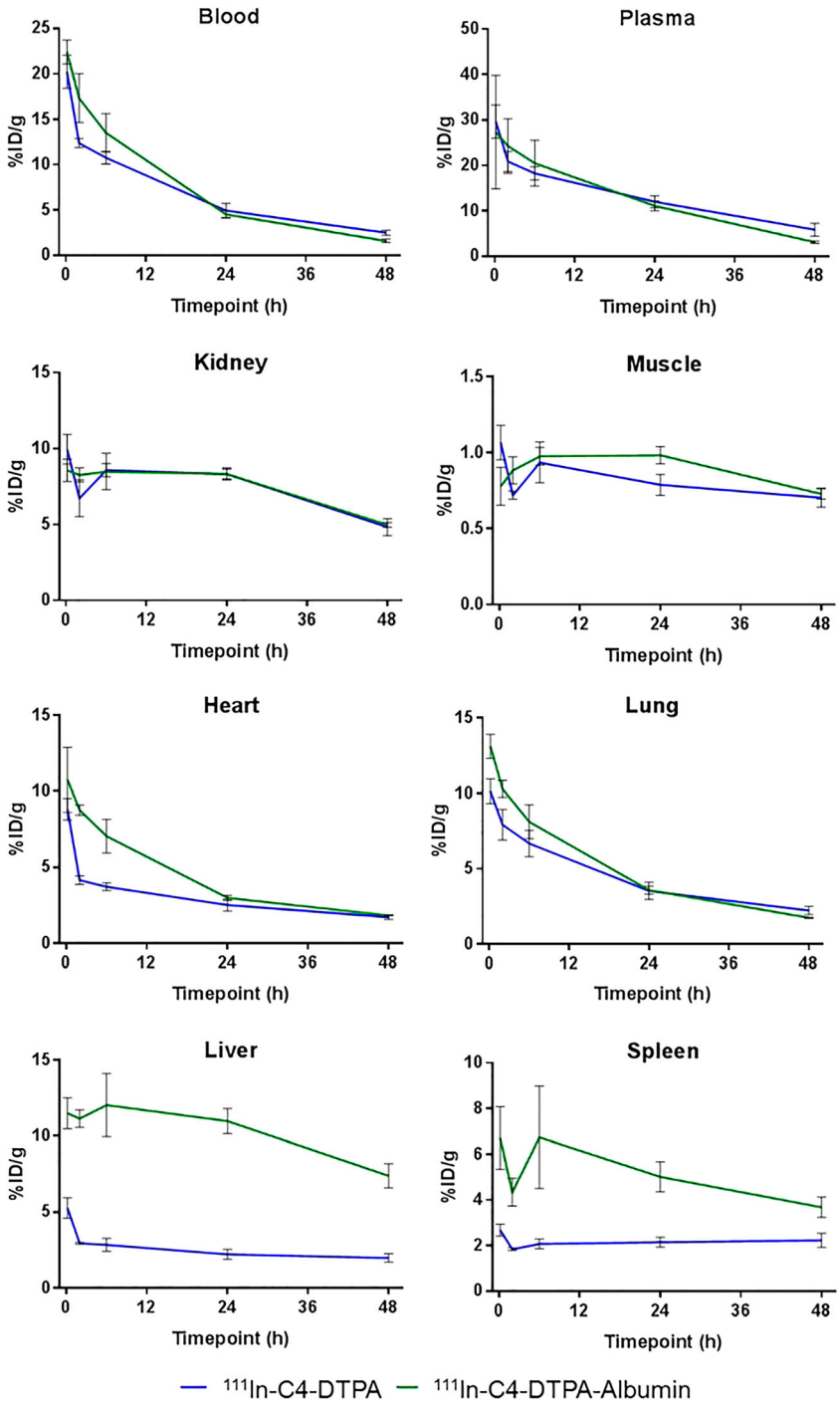

Fig. 2 Biodistribution study over 48 h in healthy nude mice ($n = 4$) treated with ^{111}In-C4-DTPA and ^{111}In-C4-DTPA-Albumin. Tissue radioactivity was determined by gamma counting. Data presented as percentages of injected dose per gram of tissue (% ID/g)

In Vivo SPECT/CT Imaging Studies in Human Tumor Xenograft Models

For the evaluation of the biodistribution and tumor uptake of the imaging agent ^{111}In-C4-DTPA in tumor-bearing mice, initial imaging studies were carried out in two human tumor xenograft models: LXFL529 (non-small cell lung cancer) and OVXF899 (ovarian cancer) with bilateral, subcutaneous implantation ($n = 8$). Tumor-bearing mice injected with ^{111}In-C4-DTPA were imaged by SPECT/CT after 1 h, 24 h, 48 h, and 72 h post-injection. At the 72-h time point, all mice were sacrificed; four mice were perfused for 3 min with saline; the other four were not perfused; samples from the blood, plasma, heart, kidneys, liver, lung, spleen, and both tumors were then collected; and radioactivity was determined by gamma counting.

Distinct radioactivity was observed in subcutaneously growing tumors of both models as can be discerned from representative 2D and 3D SPECT/CT images depicted in Fig. 3 with the bladder and kidneys being the primary elimination organ. Maximum tumor uptake was obtained at 24 h with ~ 3% ID/cm^3 (see Supplementary Material) and a higher signal-to-noise ratio was observed in the tumors at 48 h and 72 h, in the range of 3.7–5.0 (Fig. 4a). Quantitative SPECT/CT data was obtained for the left tumor only due to technical reasons (see Materials and Methods).

These results are corroborated by the results of the gamma counting at 72 h shown in Fig. 4b. Left and right tumors show 1.3–2.5% ID/g with mean tumor muscle ratios of 5.2–9.4 (Fig. 4a), and the kidneys are the only organ with higher uptake, ~ 2.6–3.8% ID/g, followed by the spleen which has values slightly below the ones measured in the tumors, 1.1–1.7% ID/g. Radioactivity in plasma was comparable to that in tumors (1.5–2.8% ID/g). No statistically significant difference was noted between the two tumor models or between perfused and non-perfused tissues, except for the heart in the LXFL529 model ($p < 0.05$ with multiple t test) indicating that radioactivity accumulation is not biased by blood in the vasculature of the organs and tumors.

In a subsequent imaging study, earlier imaging time points were added to obtain a clearer picture of the tumor accumulation profile within the first 24 h of injection. SPECT/CT images at 2 h, 6 h, 24 h, 48 h, and 72 h of four nude mice with subcutaneously implanted MAXFTN401 tumors are shown in Fig. 5a demonstrating an increasing uptake of radiolabeled albumin in the first 24 h and a slow decrease from 24 to 72 h. Figure 5b graphically depicts the kinetics of tracer accumulation quantified by SPECT in the left tumor, kidneys, liver, and muscle tissue over 72 h indicating that the maximum radioactivity in the tumor was reached after approximately 24 h (~ 3.8 ± 0.4% ID/cm^3 at 24 h compared to ~ 4.1

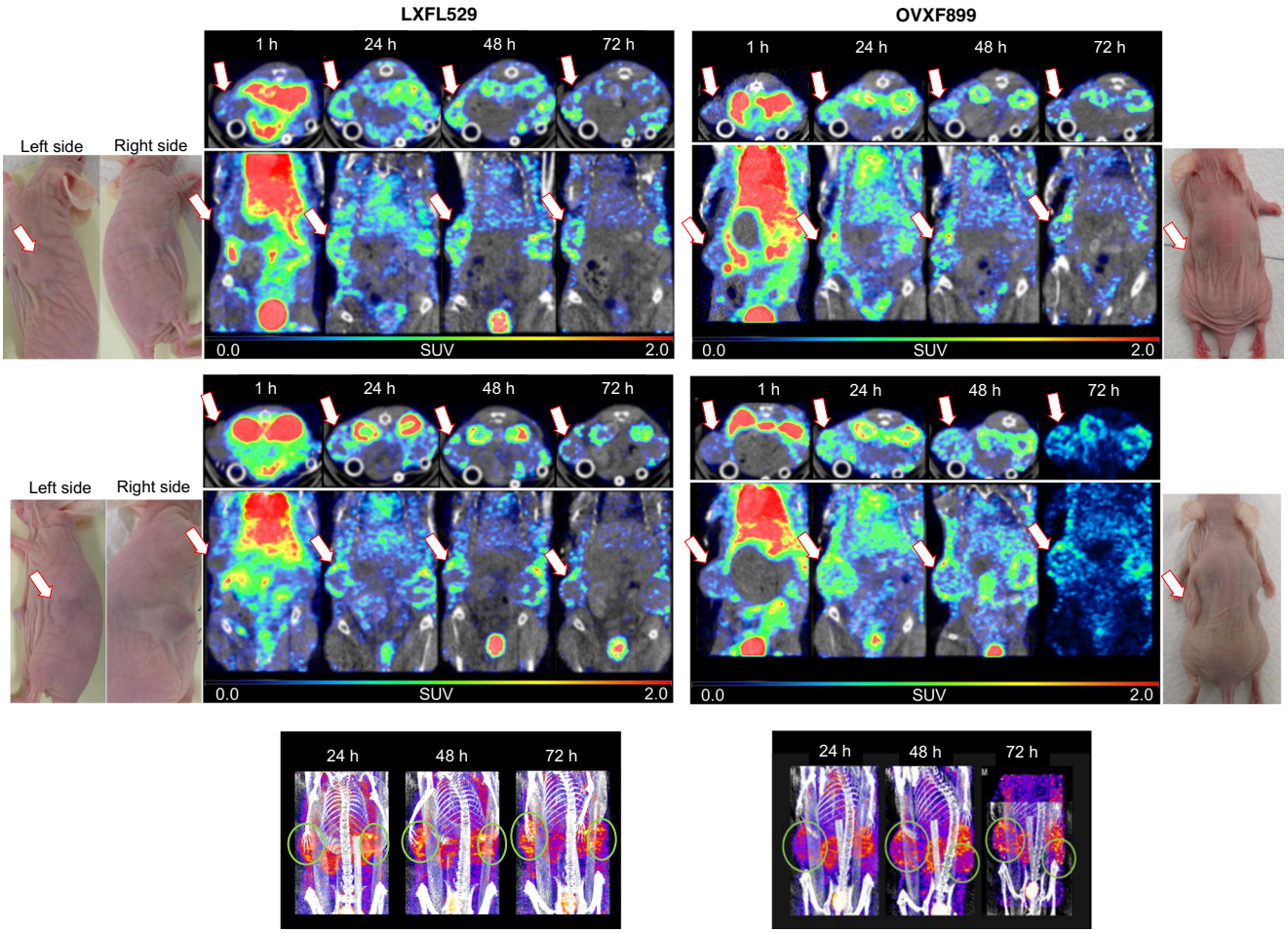

Fig. 3 Representative 2D (axial and coronal) and 3D in vivo SPECT/CT images for patient-derived tumor-bearing mice with bilateral, subcutaneously implanted lung LXFL529 (left) and ovarian OVXF899 (right) tumors treated with radiolabeled ^{111}In-C4-DTPA. Arrows and circles show left imaged tumor regions. 2D images of further tumor-bearing mice are included in the Supplementary Material

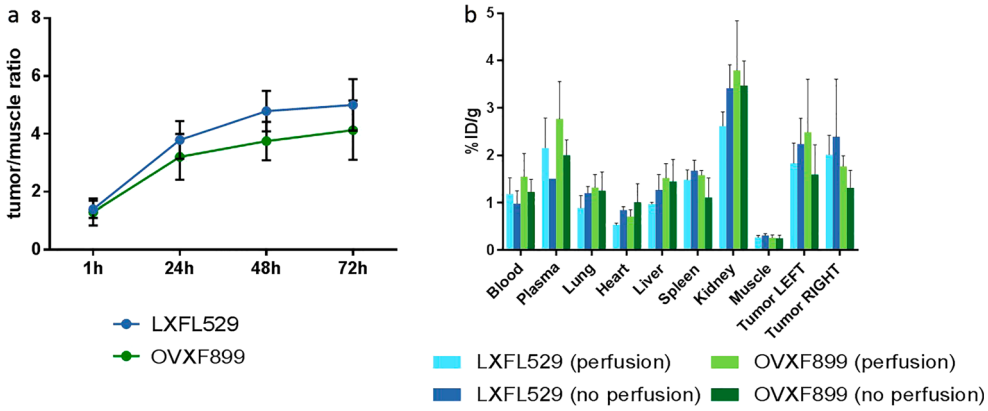

Fig. 4 ^{111}In-C4-DTPA-treated mice bearing lung LXFL529 ($n = 8$) and ovarian OVXF 899 ($n = 7$) tumors. **a** Mean tumor to muscle ratios measured with SPECT for left tumors. **b** Biodistribution results at 72 h post-injection determined by gamma counting

$\pm 0.2\%$ ID/cm^3 and $\sim 2.9 \pm 0.2\%$ ID/cm^3 for kidneys and liver, respectively). In contrast, maximal radioactivity in the kidneys and liver was already reached at 2 h or earlier ($\sim 5.8 \pm 0.1\%$ ID/cm^3 and $\sim 5.6 \pm 1.0\%$ ID/cm^3, respectively). Mean tumor/ muscle ratios were in the range of ~ 4.3 to 5.6 from 24 to 72 h post-injection. Finally, the gamma counting data at 72 h (Fig. 5c) showed a similar uptake in the tumor (~ 1.8–$1.9 \pm 0.4\%$ ID/g) compared to the two previous models (see Fig. 5). In this experiment, higher radioactivity was measured in the spleen ($\sim 2.8 \pm 0.5\%$ ID/cm^3) followed by the kidneys ($\sim 1.6 \pm 0.2\%$ ID/cm^3). Plasma radioactivity was comparable to the one measured in the tumor ($\sim 1.9 \pm 0.5\%$ ID/cm^3).

In a final experiment, we compared the biodistribution of the albumin-binding imaging agent ^{111}In-C4-DTPA with the non-albumin-binding imaging agent ^{111}In-DTPA (MAP Medical Technologies Oy) used as a negative control ($n = 4$ for ^{111}In-C4-DTPA and $n = 2$ for the negative control) in the CXF2081 tumor model. Figure 6a shows representative 2D SPECT/CT scans at 24 h, 48 h, and 72 h for the imaging agent ^{111}In-C4-DTPA, while Fig. 6b shows SPECT/CT scans at the same time points for the negative control, ^{111}In-DTPA. Mice treated with the albumin-binding imaging agent showed clear evidence of tumor uptake; in contrast, minimal radioactivity was observed with the negative control. The gamma counting data at 72 h (Fig. 6c) confirm this observation with $\sim 2.2 \pm 0.3\%$ ID/g in the tumor for ^{111}In-C4-DTPA and merely $\sim 0.07 \pm 0.03\%$ ID/g for ^{111}In-DTPA. The negative control ^{111}In-DTPA showed the lowest uptake in the tumor compared to any of the measured healthy organs. The ^{111}In-C4-DTPA biodistribution profile is similar to the one previously seen in the LXFL529 and OVXF899 tumor models, the major radioactivity being observed in the kidneys ($\sim 3.7\%$ ID/g ± 0.5) and plasma (~ 2.3 % ID/g ± 0.5) followed by the tumor.

Discussion

Tumor tissues are generally characterized by an enhanced vascular permeability and retention, a physiological property that primarily explains why macromolecules such as synthetic polymers or albumin accumulate in tumor tissue [3, 18, 19]. Serum albumin was already described to be trapped by tumors in tumor-bearing rats in the middle of the last century [20]. In the 1990s, several preclinical studies appeared in the literature demonstrating uptake of labeled albumin in tumor-bearing rodent models (reviewed in [21]). In these studies, exogenous human serum albumin was bound through free functional groups of its amino acids to an aromatic moiety [22, 23] or to a chelating agent [24, 25] and subsequently radiolabeled at the introduced moiety. The radiolabeled protein was finally purified by size-exclusion chromatography and administered intravenously to tumor-bearing animals demonstrating tumor uptake. Although this diagnostic approach identified albumin uptake in implanted tumors in rodents, it has disadvantages that include a sequence of reactions with the protein and subsequent purification steps, and additionally the administration of albumin from a foreign species (i.e., human serum albumin) to rats.

Therefore, we developed a new radio-imaging agent that binds rapidly and specifically to circulating albumin after intravenous administration, in line with our well-established drug delivery technology in which a thiol-reactive anticancer drug binds in situ to endogenous albumin [1, 2, 6–8], thus

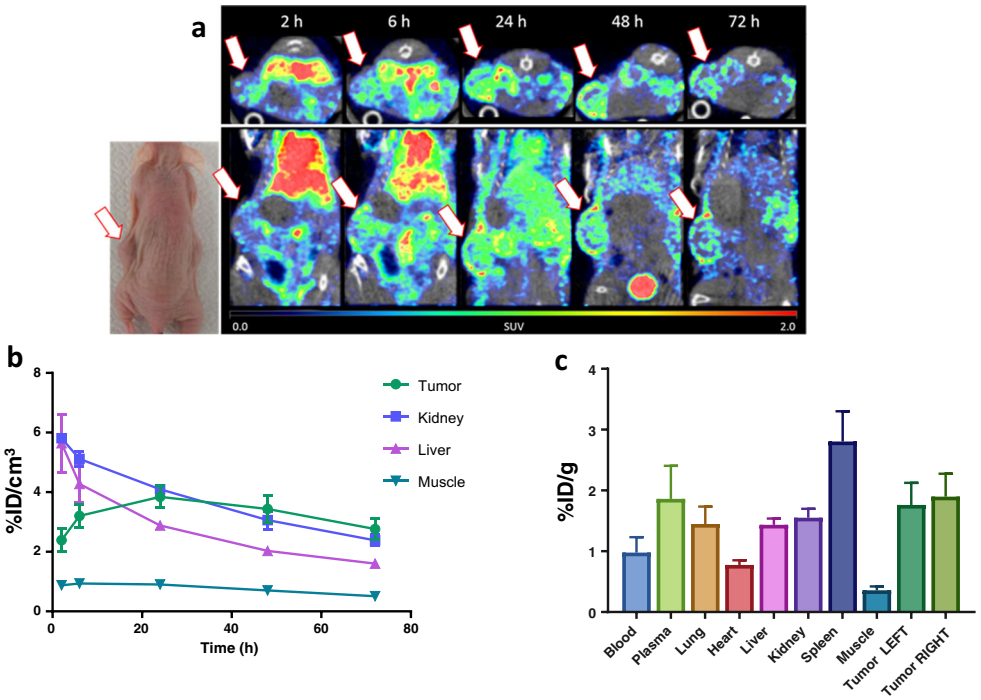

Fig. 5 Tumor-bearing mice (n = 4) with bilateral, subcutaneously implanted breast MAXFTN401 tumors treated with ^{111}In-C4-DTPA. **a** Representative SPECT/CT images (axial and coronal) at 2 h, 6 h, 24 h, 48 h, and 72 h post-injection; arrows show imaged regions of tumors implanted in the left flank. **b** Kinetics of tracer accumulation measured by SPECT in left tumors, kidneys, liver, and muscle tissue over 72 h. **c** Biodistribution results at 72 h post-injection, measured with gamma counting

avoiding protein purification and injection of a non-native albumin into rodents.

Our selected imaging agent, ^{111}In-C4-DTPA (Fig. 1), was designed to contain (a) a maleimide group as an albumin-binding moiety that binds rapidly and specifically to the amino acid cysteine-34 of circulating albumin in a Michael addition, and (b) the radioactive moiety ^{111}In-DTPA with the gamma emitter ^{111}In suitable for SPECT imaging. A major advantage of using DTPA analogs is the fact that radiolabeling of proteins occur under mild conditions.

The preparation of the DTPA derivative was achieved in a straightforward one-step synthesis and the labeling was reproducibly obtained with 98.7–99.4% radiochemical purity (a detailed description is reported in the Supplementary Material).

^{111}In-C4-DTPA was first tested in vitro in human and murine serum to confirm its albumin-binding ability and over time stability. In both serum types, immediate and quantitative binding was observed. The stability over time of the albumin-imaging agent conjugate was demonstrated in both human serum (observation period of 30 min) and mouse serum (observation period of 48 h).

In a first in vivo study, the biodistribution of the imaging agent ^{111}In-C4-DTPA was studied in healthy NMRI nude mice over 48 h and compared to that of the ex vivo labeled albumin conjugate, ^{111}In-C4-DTPA-Albumin, obtained from binding C4-DTPA to exogenous albumin and subsequent labeling with radioactive ^{111}In. Biodistribution profiles for ^{111}In-C4-DTPA and ^{111}In-C4-DTPA-Albumin differed only in the liver and spleen (Fig. 2) which is likely due to a more avid uptake by the reticuloendothelial system (RES) of ^{111}In-C4-DTPA-Albumin that was prepared from human serum albumin compared to the in situ formed albumin conjugate with endogenous murine albumin. Since no significant difference was observed in the biodistribution and the pharmacokinetic profile between the ex vivo and the in situ bound imaging agent approaches, the latter was chosen for further studies due to ease of synthesis.

In subsequent imaging studies in four human tumor xenograft models with ^{111}In-C4-DTPA (LXFL529 (non-small cell lung cancer, n = 8), OVXF899 (ovarian cancer, n = 8), MAXFTN401 (breast cancer, n = 4), and CXF2081 (colon cancer, n = 4)), we were able to show with SPECT/CT imaging and gamma counting a distinct uptake of the radiolabeled albumin in the tumors, and that tumors had a time-dependent uptake with maximum intensity noted after approximately 24 h (2.7–3.8% ID/cm^3) and a slow fall-off over 72 h (Fig. 3, 4, 5, and 6). The kidneys and bladder were the major elimination organs. Furthermore, there was no significant difference between perfused and non-perfused healthy organs or tumor in radioactivity at 72 h (Fig. 4), indicating that the uptake of in situ radiolabeled albumin is not critically influenced by the radioactivity remaining in the blood pool. Finally, the non-albumin-binding imaging agent, ^{111}In-DTPA, serving as a negative control showed no accumulation in subcutaneously growing tumors over time (Fig. 6).

A similar biodistribution profile was reported by us in the MDA-MB 435 tumor xenograft model with the albumin-binding drug aldoxorubicin labeled with ^{14}C, where uptake

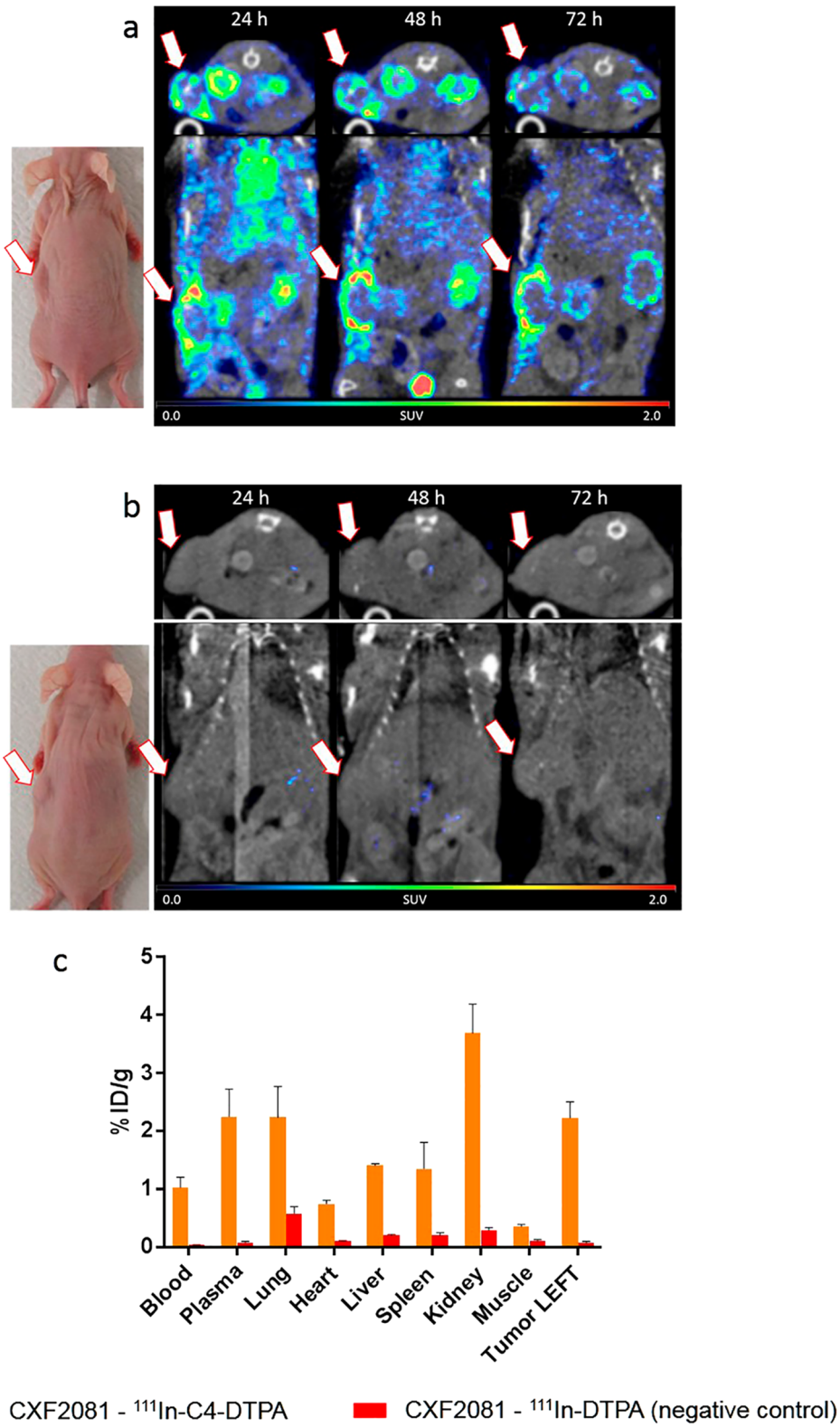

Fig. 6 Tumor-bearing mice with unilateral subcutaneously implanted colon CXF2081 tumors treated with ^{111}In-C4-DTPA ($n = 4$) and the negative control, ^{111}In-DTPA, ($n = 2$). **a** Representative SPECT/CT images (axial and coronal) at 24 h, 48 h, and 72 h post-injection of a mouse treated with ^{111}In-C4-DTPA. **b** Mouse treated with ^{111}In-DTPA as a negative control; arrows show imaged tumor regions. **c** Biodistribution results at 72 h post-injection, measured with gamma counting

in the tumor at 48 h post-injection (~ 1.5% ID/g) was comparable to the one of the albumin-binding imaging agent ^{111}In-C4-DTPA (~ 1.3–2.5% ID/g at 72 h) and the main excretion organ was the kidneys [8]. This similarity supports the application of ^{111}In-C4-DTPA as a companion diagnostic for therapy with albumin-based drug delivery systems.

Conclusion

In situ binding of the imaging agent ^{111}In-C4-DTPA to circulating albumin demonstrates a clear accumulation in the tumor substantiating the drug delivery approach of binding low molecular weight drugs to the cysteine-34 position of albumin as the drug carrier. Such an imaging agent has the potential for use in personalized medicine as a companion diagnostic for identifying patients for targeted therapy with albumin-binding drugs.

Compliance with Ethical Standards

Conflict of Interest Steffen Daum, Johannes Pall Magnusson, Lara Pes, Javier Garcia Fernandez, Serghei Chercheja, Federico Medda, Friederike Inga Nollmann, Stephan David Koester, Patricia Perez Galan, Anna Warnecke, Khalid Abu Ajaj, and Felix Kratz declare no conflict of interest.

Ethical Approval All applicable international, national, and/or institutional guidelines for the care and use of animals were followed.

Informed Consent The institutional review board of our institute approved this retrospective study, and the requirement to obtain informed consent was waived.

Publisher's Note Springer Nature remains neutral with regard to jurisdictional claims in published maps and institutional affiliations.

References

1. Kratz F, Muller I, Ryppa C, Warnecke A. Prodrug strategies in anticancer chemotherapy. ChemMedChem. 2008;3:20–53.
2. Kratz F. Albumin as a drug carrier: design of prodrugs, drug conjugates and nanoparticles. J Control Release. 2008;132:171–83.
3. Matsumura Y, Maeda HA. New concept for macromolecular therapeutics in cancer chemotherapy: mechanism of tumoritropic accumulation of proteins and the antitumor agent smancs. Cancer Res. 1986;46:6387–92.
4. Merlot A, Kalinowski D, Richardson D. Unraveling the mysteries of serum albumin-more than just a serum protein. Front Physiol. 2014;5:299.
5. Kratz F, Mueller-Driver R, Hofmann I, Drevs J, Unger CA. Novel macromolecular prodrug concept exploiting endogenous serum albumin as a drug carrier for cancer chemotherapy. J Med Chem. 2000;43:1253–6.
6. Kratz F, Warnecke A, Scheuermann K, Stockmar C, Schwab J, Lazar P, et al. Probing the cysteine-34 position of endogenous serum albumin with thiol-binding doxorubicin derivatives: improved efficacy of an acid-sensitive doxorubicin derivative with specific albumin-binding properties compared to that of the parent compound. J Med Chem. 2002;45:5523–33.
7. Mansour A, Drevs J, Esser N, Hamada F, Badary O, Unger C, et al. A new approach for the treatment of malignant melanoma: enhanced antitumor efficacy of an albumin-binding doxorubicin prodrug that is cleaved by matrix metalloproteinase 2. Cancer Res. 2003;63:4062–6.
8. Kratz F. DOXO-EMCH (INNO-206): the first albumin-binding prodrug of doxorubicin to enter clinical trials. Expert Opin Investig Drugs. 2007;16:855–66.
9. Sugio S, Kashima A, Mochizuki S, Noda M, Kobayashi K. Crystal structure of human serum albumin at 2.5 a resolution. Protein Eng. 1999;12:439–46.
10. Chawla S, Ganjoo K, Schuetze S, Papai Z, Tine BV, Choy E, et al. Phase III study of aldoxorubicin vs Investigators' choice as treatment for relapsed/refractory soft tissue sarcomas. J Clin Oncol. 2017;35:11000.
11. Chawla S, Papai Z, Mukhametshina G, Sankhala K, Vasylyev L, Fedenko A, et al. First-line aldoxorubicin vs doxorubicin in metastatic or locally advanced unresectable soft-tissue sarcoma: a phase 2b randomized clinical trial. JAMA Oncol 2015;1:1272–1280.
12. Bianchi P, Villa G, Buffoni F, Agnese G, Gipponi M, Costa R, et al. Different sites and modes of tracer injection for mapping the sentinel lymph node in patients with breast cancer. Tumori. 2000;86:307–8.
13. Maccauro M, Villano C, Aliberti G, Ferrari L, Castellani M, Patuzzo R, et al. Lymphoscintigraphy with intraoperative gamma probe sentinel node detection: clinical impact in patients with head and neck melanomas. Q J Nucl Med Mol Imaging. 2005;49:245–51.
14. Volkert W, Hoffman T. Therapeutic radiopharmaceuticals. Chem Rev. 1999;99:2269–92.
15. Wangler C, Buchmann I, Eisenhut M, Haberkorn U, Mier W. Radiolabeled peptides and proteins in cancer therapy. Protein Pept Lett. 2007;14:273–9.
16. Sugiura G, Kuhn H, Sauter M, Haberkorn U, Mier W. Radiolabeling strategies for tumor-targeting proteinaceous drugs. Molecules. 2014;19:2135–65.
17. Schmitt-Willich H, Brehm M, CL Ewers CL, Michl G, Muller-Fahrnow A, Petrov O, et al. Synthesis and physicochemical characterization of a new gadolinium chelate: the liver-specific magnetic resonance imaging contrast agent Gd-EOB-DTPA. Inorg Chem. 1999;38:1134–44.
18. Haag R, Kratz F. Polymer therapeutics: concepts and applications. Angew Chem Int Ed Engl. 2006;45:1198–215.
19. Maeda H, Wu J, Sawa T, Matsumura Y, Hori K. Tumor vascular permeability and the EPR effect in macromolecular therapeutics: a review. J Control Release. 2000;65:271–84.
20. Babson A, Winnick T. Protein transfer in tumor-bearing rats. Cancer Res. 1954;14:606–11.
21. Kratz F, Beyer U. Serum proteins as drug carriers of anticancer agents: a review. Drug Deliv. 1998;5:281–99.
22. Sinn H, Schrenk H, Friedrich E, Schilling U, Maier-Borst W. Design of compounds having an enhanced tumour uptake, using serum albumin as a carrier. Part I. Int J Rad Appl Instrum B. 1990;17:819–27.
23. Schilling U, Friedrich E, Sinn H, Schrenk H, Clorius J, Maier-Borst W. Design of compounds having enhanced tumour uptake, using serum albumin as a carrier-part II. In vivo studies. Int J Rad Appl Instrum B. 1992;19:685–95.
24. Wunder A, Stehle G, Sinn H, Schrenk H, Hoffbiederbeck D, Bader F, et al. Enhanced albumin uptake by rat tumors. Int J Oncol. 1997;11:497–507.
25. Haubner R, Schmid A, Maurer A, Rangger C, Roig L, Pichler B, et al. [(68)Ga]NOTA-galactosyl human serum albumin: a tracer for liver function imaging with improved stability. Mol Imaging Biol. 2017;19:723–30.